14th Australasian Fluid Mechanics Conference
Adelaide University, Adelaide, Australia
10-14 December 2001

The Role of Internal Waves in the Layering of Outflows from Semi-Enclosed Seas

A. A. Bidokhti[1] and R. W. Griffiths[2]

[1]Institute of Geophysics
Tehran University, Tehran, PO Box 14155-6466, IRAN

[2]Research School of Earth Sciences
Australian National University, Canberra, ACT 0200, AUSTRALIA

Abstract

Outflows from semi-enclosed marginal seas typically involve complex layered structures and inversions in vertical profiles of temperature and salinity. We have carried out experiments with turbulent plumes and their outflows in an enclosed, stratified environment. Low frequency internal waves excited by the plume outflow itself, as it intrudes into the surrounding stratification at its depth of neutral buoyancy, produce horizontal counter-flowing shear layers. These 'shearing modes' lead to branching that breaks up the outflow into a number of layers with a vertical scale determined by the structure of the upward propagating wave modes. In the oceans this scale is predicted to be of order 100m. In experiments with two diffusing components (T and S) double-diffusive convection develops thin interfaces and salt fingers between the counter-flowing layers. However, the convection is parasitic and does not generate the layers or influence their thickness. Oceanic outflows too are prone to double-diffusive convection but in this case the convecting layers, 10m to 30m thick, are potentially distinguishable from the larger 'shearing mode' structure.

Introduction

Layered structures are commonly detected in the ocean thermocline, particularly at frontal zones and intrusions from marginal seas (*e.g.* Fedorov [4]). Semi-enclosed seas, such as the Red Sea and the Persian Gulf, have "inverse estuary" flow as a consequence of excessive evaporation. This produces dense water that typically flows out over an exit sill into the ocean, where it sinks as a turbulent plume, entrains surrounding water, and intrudes into the ocean thermocline at a depth of neutral buoyancy (Bower *et al*. [3]). The vertical gradients of temperature and salinity in these outflows (or intrusions) are favourable to double-diffusive convection, which is considered to be the cause of the horizontal layering at 10-50m depth scales. There is commonly salt fingering beneath the intruding water (a T-S maximum) and "diffusive" layering above. The process has been demonstrated in laboratory experiments (Turner [7], Ruddick & Turner [6]). However, we note that coarse vertical structure on the scale of 50-100m is observed in ocean outflows (Fig. 1) and it is not clear that this is a result of convection.

It has recently been shown that the outflow from a dense turbulent plume in a long channel excites a series of strong counter-flowing horizontal shear layers (Wong *et al.* [9]). These were explained in terms of low frequency internal gravity waves that carry energy and momentum upward from the outflow level. The vertical scale can be predicted by a matching of the downward phase speed of low-frequency travelling internal waves with the upward advection speed throughout the tank associated with the displacement by the entrained volume flux in the plume. The matching leads to the excitation of a preferred wave number. The number of layers observed in experiments is 4 to 6 (between the top of the density gradient at the plume source and the base of the tank). Long-period internal gravity waves with nearly vertical wave number vectors have also been suggested as the cause of multiple horizontally-coherent layers observed below the upper ocean mixed-layer (Fedorov [4], chapt. 5).

Here we present results of laboratory experiments with outflows generated by turbulent buoyant plumes falling into stratified environments such that the outflow is at intermediate depths rather than on the bottom of the tank. This places constraints on the density difference between the plume and its environment but allows us to use a variety of density gradients that are independent of the plume properties. Importantly, we use both single-component flows and two-component (double-diffusive) cases to investigate the relative roles in layer formation of internal waves and double-diffusive convection, and interactions between these two processes.

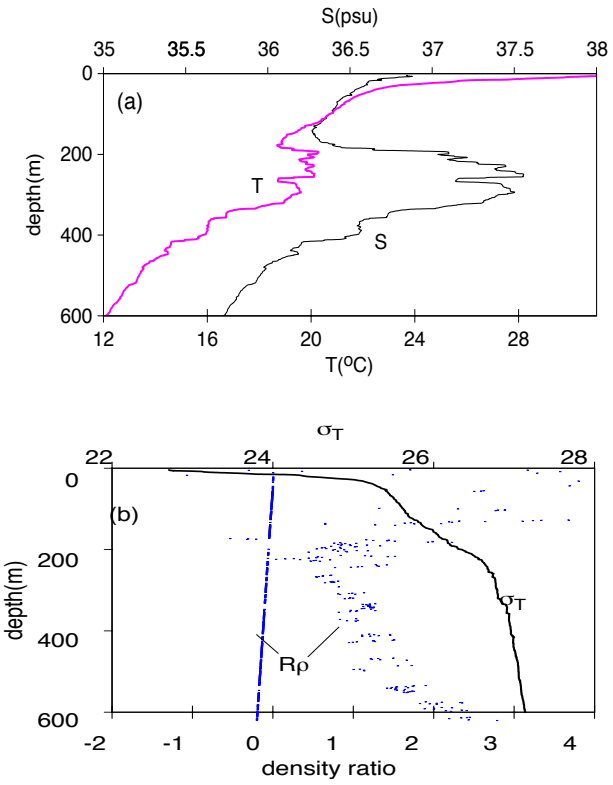

Figure 1. Vertical profiles through the Persian Gulf outflow at (57.06 Long., 24.37.8 Lat.) for summer (1992): a) Temperature and Salinity; b) Potential density (σ_T) and density ratio $R_\rho = \alpha T_z/\beta S_z$. Profiles are shown to a depth of 600m (data from NOAA Mt. Mitchell Cruise). Density ratios $R_\rho > 1$ are salt finger favourable, $0 < R_\rho < 1$ are favourable to 'diffusive' interfaces, $R_\rho = 0$ is uniform temperature, and for $R_\rho < 0$ both T and S are stably distributed.

Experimental set-up

The experiments were carried out in a glass channel 1.80m long x 0.15m wide x 0.30m deep (Fig. 2). This tank was stratified with a sugar or salt concentration gradient. Two

types of density profile were used: a non-linear 'filling-box' density gradient (produced by a turbulent dense plume, Baines & Turner [1]) or a linear density gradient (produced by filling onto a floating porous 'float from a stirred bucket of dense solution connected to a bucket of fresh water). For the "filling-box" gradient the stratifying plume source, placed at $H = 0.2$m above the bottom of the tank, supplied a buoyancy flux $F^* = Qg'$, where $g' = g\Delta\rho/\rho$, the reduced gravity of the plume, and Q is the source volume flux. The initial profile of buoyancy frequency $N(z)$ was calculated from the theoretical "filling-box" solution [1]. For both stratification types, we left the gradient to settle for several hours.

A source of dyed salt or sugar solution, placed at one end of the long tank and equidistant from the side walls, was later turned on. This plume had a buoyancy flux F' chosen to produce an outflow (or intrusion) at intermediate depths. (The initial penetration depth Z of the outflow was estimated from $Z = 5(F'/\pi)^{1/4}N^{-3/4}$, Turner [7]). In each case F' was chosen such that $Z \approx H/2$, where H is the depth of stratified fluid beneath the plume source. Experiments were run for both the single component case (a salt plume into a salt gradient) and for the two-component (double-diffusive) case (generally salt into sugar, but for a few cases sugar into salt).

Horizontal velocities were revealed by dropping dye crystals that formed initially vertical traces, and video recording the flow. A conductivity probe was used to take vertical salinity profiles.

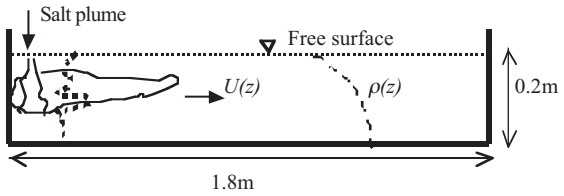

Figure 2. A sketch of the experimental set-up.

Results and discussion

The non-dimensional parameters governing the flow in the single component (say, T) case are the Prandtl number $Pr = \nu/\kappa_T$ (where ν is the kinematic viscosity and κ_T is the diffusivity of component T), the aspect ratios H/L and H/W (where L and W are the length and width of the tank, respectively) and the dimensionless plume buoyancy flux $F_P = F'/(H^4N_0^3)$. Here the buoyancy flux $F' = q\Delta\rho g/\rho$, where q is the volume flux of the plume source and N_0 is the buoyancy frequency of the environment. In the case of a stratification produced previously by a plume we use $N_0 = N(z = H)$ (where z is measured downward from the plume source) and N is dependent on the strength F^* of the stratifying plume. In addition, the relative magnitudes of forcing and molecular dissipative processes are described by either the Peclet number $Pe = F'^{1/3}H^{2/3}/\kappa_T$ or a similar Reynolds number.

For two-component cases we require three new parameters: the density ratio $R_{\rho P} = \alpha\Delta T/\beta\Delta S$ (where ΔT and ΔS are property differences between the plume source and the bottom of the tank stratification, and α and β are the coefficients of density change due to T, salt, and S, sugar, respectively); the ratio of S and T diffusivities $\tau = \kappa_S/\kappa_T$, and a measure of convective dissipation, such as a Rayleigh number. However, in place of the Rayleigh number we choose the ratio $F_C \equiv F_{DS}/F_S'$, which compares the vertical S-flux (F_{DS}) due to double-diffusive convection over the area LW to the plume source salt flux ($F_S' = q\Delta S$). Assuming the usual high-Rayleigh number result $F_{DS} \sim 0.1\, f(\tau, R\rho)\, (g\beta\kappa_S^2/\nu)^{1/3}\, (\Delta S)^{4/3}(LW)$ [7] (R_ρ the local stability ratio) and dropping the dependence on τ and R_ρ (which can be accommodated in those two parameters) we write

$$F_C = 0.1\kappa_S^{2/3}(\beta\Delta S\, g/\nu)^{1/3}q^{-1}(LW).$$

Typical values of F_P and F_C in our two-component experiments are of order 0.02 and 10, respectively, with $R_{\rho P} = 1$, whereas in single component runs $R_{\rho P} = 0$ and $F_C = 0$. We estimate that the corresponding values for the Persian Gulf or Red Sea outflows are of order $R_{\rho P} \sim 1$, $F_P \sim 0.14$ and $F_C \sim 100$, respectively (the latter based on $L \sim 100$km, $W \sim 10$km). The large value of F_C indicates that once the outflow extends over a large horizontal area the vertical double-diffusive fluxes can be large compared to the plume salt flux at its source level. Convective fluxes might potentially then play a role in shaping the structure of the outflow. The experiments of Turner [6] with a two-component source at its neutral buoyancy level had $F_P = F' = 0$ and very large F_C.

Visualisations of the two-dimensional laboratory flows showed that the plume outflow began to intrude into the gradient at the level of neutral buoyancy. The rate of advance of the leading edge of the outflow initially increased with time, while the intrusion became thicker. The intrusion later split, with a new layer growing beneath the main intrusion. The plume flux created a "filling-box" circulation that added density to the entire water column above the level of the outflow. This in turn caused both the maximum penetration depth of the plume and the outflow depth to increase with time. The sequential formation of new layers was repeated until the dyed outflow filled the entire depth of the tank. The formation of each new layer was accompanied by a reduction (and sometimes a reversal) of the spreading rate of the previous layer.

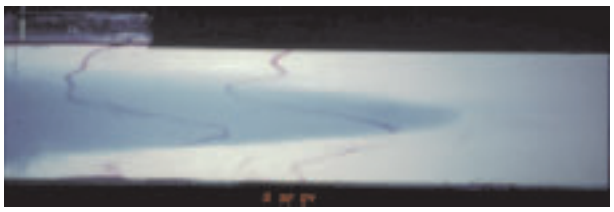

Figure 3. Displacement of vertical dye lines indicating the velocity profile produced by the single-component outflow from a *salt* plume in a "filling box" gradient of *salt* solution. $F^* = 6.0\text{x}10^{-7}\text{m}^4\text{s}^{-3}$, $F' = 0.8\text{x}10^{-7}$ m^4s^{-3}, $F_C = 0$. Similar velocity profiles are seen ahead of the outflow. About 1/2 of the length is shown here.

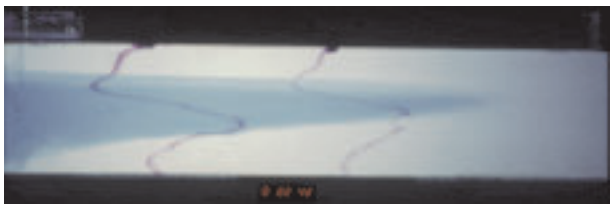

Figure 4. Displacement of vertical dye lines indicating the velocity profile produced by the outflow from a salt plume in a "filling box" gradient of sugar. $F^* = 6.0\text{x}10^{-7}\text{m}^4\text{s}^{-3}$, $F' = 0.8\text{x}10^{-7}\text{m}^4\text{s}^{-3}$, $F_C = 12.4$. Double-diffusive convection contributes to the internal recirculation in layers, with salt fingering within and above each layer.

Typical velocity profiles observed within the outflows are shown in Figures 3 and 4 for single component and double-diffusive cases, respectively. Similar profiles were seen in the surroundings ahead of the outflow. The velocity structure in both cases was consistent with that of the low-frequency 'shear modes' previously observed for a plume falling into a "filling-box" gradient, where the dense outflow was along the bottom of the tank [9]. The primary differences in our case are that: 1) the shear layers were confined to the regions within and above the outflow, and 2) the dyed outflow water was wedged-shaped with a sloping interface beneath. The velocity

amplitude of the shear layers decayed rapidly with height, particularly in the case of "filling-box" density gradients. We attribute this rapid spatial decay to the small plume buoyancy fluxes (hence small Reynolds numbers) to which we were restricted by the weak density gradient. Because the internal intrusion is bounded below by stratified fluid instead of a solid boundary, some internal wave energy can propagate downward into the underlying stratification. However, we saw no evidence of this at low frequencies.

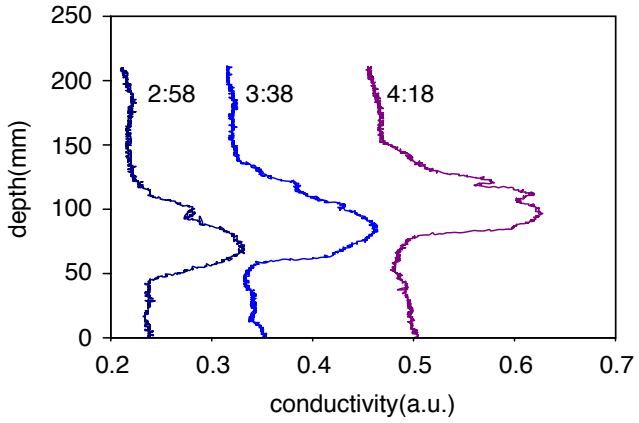

Figure 5. Conductivity profiles at x = 1.2m from the plume at different times (hr:min.) for a salt plume outflow intruding into a sugar "filling box" gradient ($F' = 0.25\text{x}10^{-7}\text{m}^4\text{s}^{-3}$, $N_0 = 0.31\text{s}^{-1}$, $F_C = 20.9$). The initial gradient was produced by a sugar plume having $F^* = 3.0\text{x}10^{-7}$ m^4s^{-3}. Units are arbitrary and profiles have been shifted by 0.1 or 0.2 units in order to avoid overlapping.

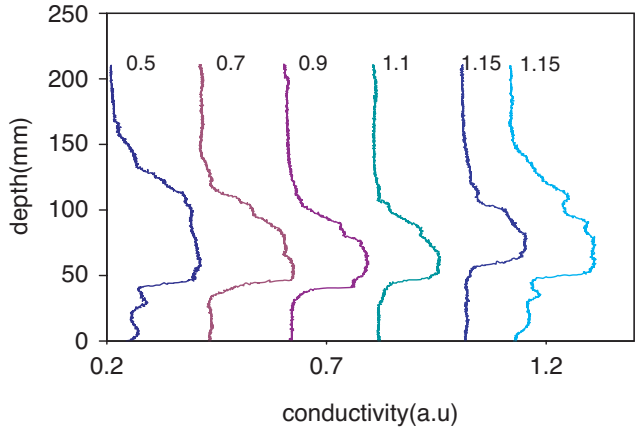

Figure 6. Conductivity profiles at different positions (x in meters, all taken at 2hr:50min, excepting the last profile, at 3hr:50min) for a run having the same conditions as Figure 5 (salt into sugar).

The counter-flowing shear layer structure at and above the outflow level was similar in both the single and two component cases. Hence double-diffusive convection was not the cause of the layering, which we again attribute to low-frequency vertically propagating waves. Indeed, the frequency of layer formation and the vertical length scales were not influenced significantly by the addition of strong convection. The formation of the shear layers led to 'inversions' of T and S at smaller scales than the full depth of the outflow and this may have promoted stronger double-diffusive convection. In return, double-diffusive convection acted on the vertical salt and sugar gradients in a largely parasitic manner. Where S was stabilising the convection sharpened the gradients (forming 'diffusive' interfaces). Where S was destabilising, salt fingering was active and S and T gradients tended to be reduced and spread vertically. The resulting convective fluxes tended to shift the noses of double-diffusive intrusions across density surfaces (downward when salt fingers were on the top) with both time and distance from the plume. However, upward advection forced by the outflow volume flux also implied that density surfaces and convecting layers were carried upward through the horizontal velocity structure of the shearing modes and this displacement tended to overwhelm the effect of the convective fluxes.

Figures 5 and 6 show the conductivity profiles associated with a two-component outflow into an initial "filling-box" gradient (salt plume into sugar gradient) at different times and distances from the plume, respectively. This case had salt fingering above the intrusion. Hence the broader mean conductivity (or T) gradient above the intrusion was a result of finger fluxes and the upward transport of salt was a result of the upward "filling-box" advection. Evidence can be seen for layering within the intrusion. Although layers appear as small features in the conductivity profiles, they corresponded to density interfaces and convecting layers visible on a shadowgraph screen. On the other hand, snapshots show little correspondence of the layering in conductivity and density to the horizontal velocity structure. The relationship between these can be seen only in the time evolution, where new layers were formed while the outflow was advected upward through the quasi-steady shear layers, or where the plume penetration depth increased and forced the structure of the shear layers to evolve.

Figure 7 shows conductivity profiles for an outflow from a much stronger (x 12) salt plume into a larger (x 4) *linear* sugar gradient compared to figure 5. Again there was strong salt finger convection above the intrusion and diffusive interfaces beneath each layer. In this case the larger plume buoyancy flux led to a faster evolution and to a large increase of the penetration depth with time. The larger concentration contrasts caused the double-diffusive convective fluxes to be greater, contributing to the larger vertical spreading of the outflow. Again the small features in the conductivity profiles are real and corresponded to convecting layers. Conductivity records at fixed points in the intrusion also revealed the presence of low frequency internal waves [2].

Figure 8 shows density profiles for a single component experiment with a salt plume outflow into a linear salt gradient, but otherwise similar to that of Figure 7. The saline environment in this case contributed an underlying gradient in conductivity and density, and these make the signature of the outflow less distinct than in conductivity profiles for experiments using a sugar environment (hence our focus on the latter case). However, they show the addition of density to the water column above the outflow level and the consequent deepening with time of the plume penetration. The deepening of the outflow is slightly less than in the double-diffusive case of Figure 7, a difference that is possibly a result of the added downward flux of density due to double-diffusive convection in that case. As previously noted by Wong *et al.* [9], the internal shear modes involve only very small perturbations to the density field and so are not visible in Figure 8, despite their obvious appearance in profiles of horizontal velocity.

Ocean outflows

There are a number of qualitative similarities between the laboratory flows and data for ocean outflows from marginal seas. In particular, both appear to contain coarse density and velocity structure on scales only slightly smaller than the full thickness of the outflow. The intrusions are broken into a small number of layers. In addition, the full depth of the intrusions appears to scale in a similar manner when compared to the depth Z from the sill (or plume source) to the

base of the intrusion. Both in laboratory and ocean examples, the intrusion thickness is roughly 0.3 to 0.5 Z, after subtracting the background stratification. Wong *et al.* [9] found a similar result for the depth of a dense plume outflow at the bottom of a tank. In that case the outflow depth was approximately 0.2 to 0.3 Z and was controlled by the vertical wave number of upward propagating internal waves. The quantitative difference is not surprising because intrusions at intermediate-depths have the rigid bottom boundary replaced by a stratified region.

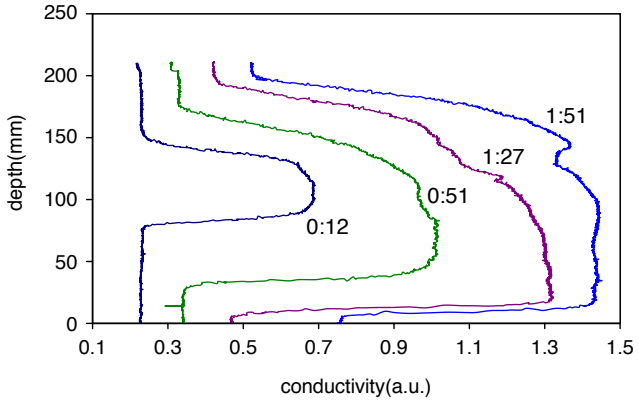

Figure 7. Conductivity profiles taken closer to the plume (x = 0.6m) than those in Figure 5 and for an experiment with a very strong salt plume outflow into a *linear* sugar gradient (F' = 3.0x10^{-7}m^{4}s^{-3}, N = 0.65s^{-1}, F_C = 3.6). The numbers on the graphs show time in hours: minutes.

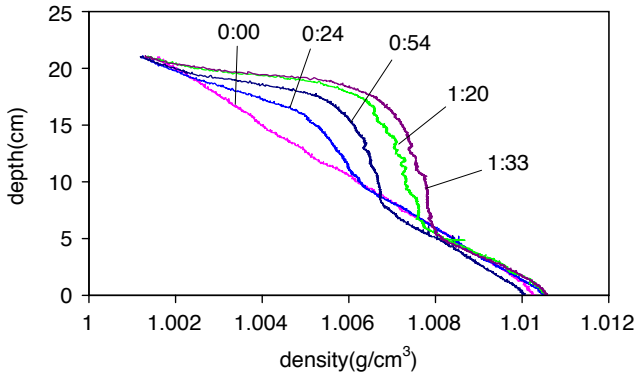

Figure 8. Absolute density profiles obtained from conductivity at x = 0.6m from the plume for a *single component* experiment (a salt plume outflow into a *linear* salt gradient, F' = 3.0x10^{-7}m^{4}s^{-3}, N = 0.65s^{-1}). The numbers show time in hours: minutes.

Elsewhere (Bidokhti & Griffiths. [2]) we have estimated the vertical length scales and horizontal fluid velocities of the internal shear modes that might be produced by the Persian Gulf and Red Sea outflows, using the theoretical model of Wong *et al.* [9] and the estimated buoyancy fluxes over the sills. The vertical scale is predicted to be of order 100m and the velocity of order 0.1ms^{-1}. This thickness is much greater than the convecting layer thicknesses of order 10m commonly attributed to double-diffusive convection. Hence there is potential for discrimination between the two. There is no such scale separation in the laboratory experiments, where convection does not form additional smaller layers but only modifies the flow within the shear layers. An estimate of the rate of decay with height of the velocity amplitude of shear modes (resulting from friction based on the turbulent eddy viscosity $\nu = 10^{-4}$m^{2}s^{-1}) gives a decay height of order 100m. When normalised by the thickness of the shear modes or the depth from the source, this depth is similar to the decay height observed and predicted in our laboratory experiments (where we use the molecular viscosity). Further analysis of the decay of low frequency internal waves due to viscosity is given by Hughes [5]. It is not clear from our experiments what mechanism determines the frequency of layer formation, though it may relate to the very long period oscillation in shear mode structure reported by Wong *et al.* [9].

We note that the actual outflows are three-dimensional and that for semi-enclosed seas or gulfs the appropriate values of the length and width of the basin are uncertain. There are also Coriolis forces and frictional effects due to much smaller aspect ratios in the oceans, both of which tend to impose limitations on the horizontal scales. Hence we have used as L the length of the intrusion itself (~100km), under the assumption that friction will effectively limit the horizontal scale of internal wave motions at the very small aspect ratios (<0.001) relevant in the ocean. We have also taken W to be the width of the intrusion (~10km), despite this being an order of magnitude greater than the internal Rossby radius. These large lateral scales lead to the large value of the dimensionless convective flux, $F_c \sim 100$.

Conclusions

Laboratory experiments on intrusions generated by turbulent plumes into stratified environments show that low frequency internal waves are excited by the intrusion and can drive counter-flowing shear layers. These 'shearing modes' may be responsible for branching of the intrusion into a small number of deep layers that have much larger vertical scales than those resulting from double-diffusive convection. Both scales are observed in ocean outflows, whereas these two scales are similar in the laboratory. The potential role of convection depends largely on the ratio of vertical convective fluxes within the outflow to the plume (sill) buoyancy flux. By comparing single- and two-component cases we conclude that double-diffusive convection is parasitic on the shearing modes in the experiments, modifying the details of density structure and contributing to vertical fluxes without altering the thickness of the dominant layers.

Acknowledgments

AAB acknowledges financial support from Tehran University for sabbatical leave at ANU. We thank T. Beasley and R. Wylde-Browne for their technical assistance.

References

[1] Baines, W. D. and Turner, J. S., Turbulent buoyant convection from a source in a confined region, *J. Fluid. Mech*., **37**, 1969, 51-80.

[2] Bidokhti A. A. and Griffiths, R. W., Low frequency internal waves and the layering of outflows from semi-enclosed seas. 2001, *J. Geophys. Res*., in preparation.

[3] Bower, A. S., Hunt, H. D. and Price, J. F., Character and dynamics of the Red Sea and the Persian Gulf outflows, *J. Geophys. Res*., **105**, 2000, 6387-6414.

[4] Fedorov, F. N., *The Thermohaline Finestructure of the Ocean*, Translated by D.A. Brown, Ed. J. S. Turner, Vol 2, Pergamon Marine Series, 1978.

[5] Hughes, G. O., Damping of internal gravity waves in stratified fluids, *Proc. 14th Aust. Fluid Mech. Conf*., in press.

[6] Ruddick, B. R. and Turner, J. S., The vertical length scale of double-diffusive intrusions, *Deep Sea Res*., **26A**, 1979, 903-913.

[7] Turner, J. S., Double-diffusive intrusions into a density gradient, *J. Geophys. Res*., **83**, 1978, 2887-2901.

[8] Turner, J. S., *Buoyancy Effects in Fluids*, Cambridge University Press, New York, 1973.

[9] Wong, A. B. D., Griffiths, R. W. and Hughes, G. O., Shear layers driven by turbulent plumes, *J. Fluid Mech*., **434**, 2001, 209-244.